Journal Name

Dynamic Article Links ►

Cite this: DOI: 10.1039/c0xx00000x

www.rsc.org/xxxxxx

ARTICLE TYPE

Carbonization over PFA-Protected Dispersed Platinum: An Effective Route to Synthesize High Performance Mesoporous-Carbon Supported Pt Electrocatalyst

Fujun Li, Kwong-Yu Chan* and Hoi Yung

Received (in XXX, XXX) Xth XXXXXXXXX 20XX, Accepted Xth XXXXXXXXX 20XX
DOI: 10.1039/b000000x

An alternative and effective route of synthesizing mesoporous carbon supported Pt nanoparticles is introduced. In reverse order to the conventional synthetic route, carbonization occurs after dispersion of platinum. In this process, H_2PtCl_6 acts as a Pt source and also serves as a catalyst for the polymerization of furfuryl alcohol (FA). The polymerized FA around the H_2PtCl_6 nanoparticles functions as a procteting agent and prevents the growth of Pt nanoparticles in the later high temperature carbonization step. The resulting Pt nanoparticles are highly dispersed in the mesoporous carbon structure, CMK3, and give a much higher methanol oxidation current when compared with Pt/CMK3 electrocatalyts prepared via the conventional route.

Introduction

Carbon supported platinum remains the most versatile electrocatalyst for low temperature fuel cells. Active investigations are made to optimize the structure of the electrocatalyst for maximum activity and stability.[1,2] Apart from the metal nanostructure, the porous carbon support structure can be equally important as it enables metal dispersion, efficient transport of reaction species, and conduction of electrons and heat. While Vulcan and other activated carbons have been commonly used, they do not have uniform and well-defined structural properties for definitive investigations. The ordered mesoporous carbons (OMC), e.g. CMK3 carbon,[3] provide well-defined and high performance structures for electrocatalysts studies. There are increasing uses of OMC as supports for platinum[3] and platinum containing mixed-metal catalysts.[4-7]

A typical synthesis of carbon supported platinum electrocatalyst involves loading a platinum source into an existing porous carbon structure. A synthetic porous carbon, e.g. ordered mesoporous carbon would be created first. Using CMK3 as an example of carbon support, Route A in Scheme 1 shows the conventional synthesis of porous-carbon supported Pt nanoparticles. An ordered mesoporous silica is first filled with a carbon precursor and catalyst in step i,[10] followed by carbonization in step ii, removal of silica in step iii, and loading of metal nanoparticles into the OMC in the last step. The same procedure is used to load other metal nanoparticles[7-9,11] and into other porous carbons.[12,13] The platinum nanoparticles can be deposited from a precursor using the glycol method,[14,15] reducing agents,[16] or microemulsions.[17]

The last step of loading metal nanoparticles into an OMC structure encounters several difficulties. The long and narrow carbon mesopores hinder penetration of metal precursors, e.g. colloidal metal prepared from glycol[14,15] or metal containing microemulsion.[17] The partially hydrophobic pores of OMC also prevent complete wetting by aqueous metal precursors. These lead to non-uniform dispersion of metal nanoparticles and losses of metal precursors in the synthesis. High metal loading in OMC cannot be routinely achieved. For multiple metals, control of metal ratio at nanoparticle level is also rarely achieved due to differences in wettability, penetration, and deposition kinetics of metal precursors. Furthermore, remains of carbonization catalysts e.g. sulfur from sulfuric acid or aluminum can be detrimental to the performance of electrocatalysts. These problems of loading metal nanoparticles are common to other porous carbons, e.g. Vulcan carbons.

Metallization before or during carbonization has seldom been considered since the high carbonization temperature ≥ 700 ºC destroys nanoparticle-protecting agents and encourages uneven and unrestricted growth of metal particles. A previous attempt to carbonize platinum-loaded mesoporous silica resulted in large and non-uniformly sized Pt particles.[8] We demonstrate here, however, the feasibility of a reverse order synthesis with H_2PtCl_6 added before carbonization. Using Pt/CMK-3 as an example, the reverse order synthesis is shown in Route B of Scheme 1. In this alternative route, H_2PtCl_6 does not only provide the source of Pt but also serves as a catalyst for the polymerization of furfuryl alcohol (FA). At the same time, the polymerized FA (PFA) around the surface of H_2PtCl_6 nanoparticles, functions as a protecting agent and prevents the growth of Pt nanoparticles in the high temperature (>700°C) environment of a subsequent carbonization step. We denote this route as “carbonization over PFA-protected dispersed platinum” (CPDP). Table 1 lists the steps of the two alternative routes and the structures before and after each reaction step.

Cite this: DOI: 10.1039/c0xx00000x

www.rsc.org/xxxxxx

ARTICLE TYPE

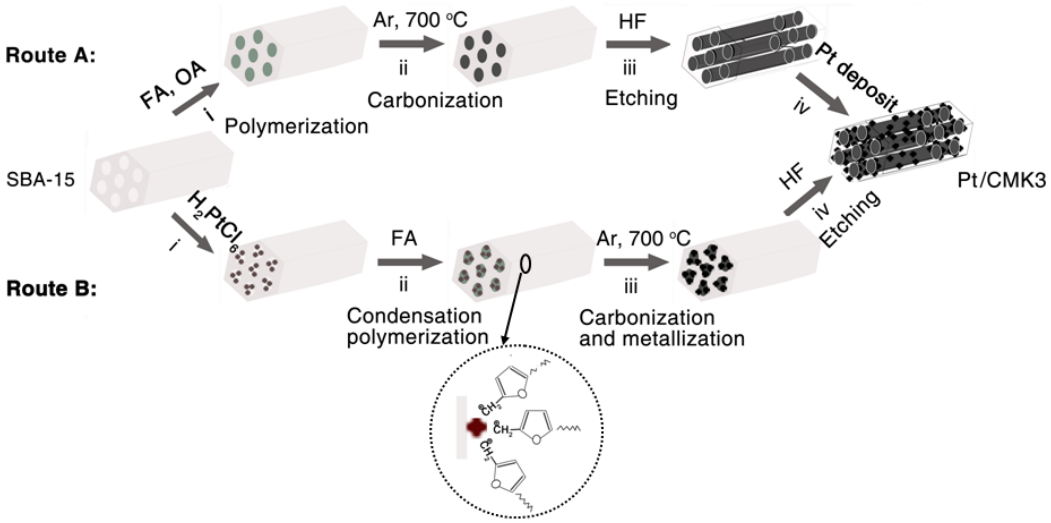

Scheme 1. Synthetic pathways for Pt nanoparticles supported on OMC via the conventional method and the proposed CPDP strategy. The exploded and circled region illustrate protection of the Pt source by the polymerized FA.

Table 1 Comparison of alternative routes of synthesizing porous carbon supported platinum nanoparticles.

Route	Structure	Step i	Structure	Step ii	Structure	Step iii	Structure	Step iv	Structure
A	SBA-15	filling FA catalyst, heating	PFA filled SBA-15	carbonization at 700 ºC	carbon filled SBA-15	HF etching	CMK3	Pt loading	Pt/CMK3-EG
B	SBA-15	filling H_2PtCl_6	H_2PtCl_6 nanoparticles dispersed in SBA-15	FA addition and condensation polymerization	PFA encapsulated H_2PtCl_6 nanoparticles in SBA-15	Carbonization metallization	carbon filled SBA-15 with Pt nanoparticles	HF etching	Pt/CMK3-CPDP

[a]

Though a common Pt/CMK-3 final structure is shown for the two routes, Route B leads to Pt nanoparticles that are better dispersed. In other reported syntheses[5,18] with metallization and carbonization proceeding simultaneously at high temperature, different platinum precursors, including platinum acetylacetonate and $(NH_3)_4Pt(NO_3)_2$ are used without a protecting agent to preserve dispersion and prevent growth of platinum nanoparticles. Carbonization occurs around an added catalyst, such as oxalic acid,[13,18] or sulfuric acid[5,8] rather than a H_2PtCl_6 site in the CPDP route. Details of the CPDP synthesis, characterization of the resulting Pt/CMK3 structure, and electrocatalytic activity for methanol oxidation are presented in this paper.

Experimental

Synthesis of SBA-15 and CMK3

The ordered mesoporous silica was prepared by the procedure described in reference 10. Briefly, 1.0 g of triblock ethylene oxide (EO)-propylene oxide (PO)-EO copolymer P123 ($EO_{20}PO_{70}EO_{20}$, M = 5800, BASF) was dissolved in 40 ml of 1.6 M HCl solution at 35 ºC. Then 2.2 g of tetraethylorthosilicate (TEOS, 98 %, Aldrich) was added under stirring. The mixture was kept at 35 ºC, stirred for 1 day, transferred into an autoclave and heated to 90 ºC for another 2 days. The product was collected by centrifugation and dried at 80 ºC overnight. P123 was burnt off at 550 ºC for 5 hrs in flowing air to yield the product SBA-15. Furfuryl alcohol (FA) and oxalic acid with a molar ratio of 30 to 1 were filled into SBA-15 by an incipient wetness impregnation method. The composite was heated to 80 ºC and then 160 ºC for 3 hrs to promote the polymerization of FA. After that, the as-synthesized composite was carbonized at 700 ºC in flowing Ar for 3 hrs. Then the template SBA-15 was removed in 10 wt% HF solution.

Synthesis of Pt/CMK3-EG

45 mg of CMK3 was stirred into a solution of ethylene glycol (EG) containing 5 mg of Pt in $[PtCl_6]^{2-}$, and the pH was adjusted to 13 by using 0.1 M of NaOH in EG. The solution was heated to

130 ºC for 3 hrs with flowing N_2. The product Pt/CMK3-EG was collected by centrifugation, then washed with de-ionized water for several times and dried at 80 ºC in a vacuum oven.

Synthesis of Pt/CMK3-CPDP

0.3 g of SBA-15 was dispersed into 60 ml of CH_2Cl_2, then 0.312 ml of water and ethanol solution (1:1, v/v) containing 8.84 mg Pt in H_2PtCl_6•xH_2O was added. The pH of the solution is between 1.0 and 2.0. The mixture was stirred overnight, filtered, and dried in a vacuum oven at 60 ºC for 12 hrs. After cooling down, 0.312 ml of FA was impregnated into the H_2PtCl_6•xH_2O/SBA-15 composite stored in a refrigerator. The colour of the composite changed from dark brown to green and then dark green at room temperature. Left in room temperature condition overnight, polymerized FA (PFA) attached H_2PtCl_6•xH_2O in SBA-15 was placed in flowing Ar at 700 ºC for 3 hrs for carbonization to complete.

Characterization

Scanning transition electron microscopy (STEM, Philips TECNAI 20 with a 200 kV accelerating voltage) and high resolution transition electron microscopy (HRTEM, JEOL 2010-F) were used to characterize the structures of the as-synthesized SBA-15 and CMK3 with and without Pt deposition. Nitrogen sorption isotherms were obtained on a Micromeritics ASAP 2020 analyzer at 77 K. The surface area was determined by using the Brunauer-Emmett-Teller (BET) method and the pore size distribution was calculated via the Barrett-Joyner-Halenda (BJH) method. The total pore volume was obtained at a single point of P/P_0 = 0.97. Raman Spectroscopy was carried out using a Renishaw Invia Raman Microscope (Renishaw, UK) with He-Ne laser (633 nm, 25 mW). Thermo-gravimmetric analysis (TGA) performed in air on a NETZSCH TG 209 F3 instrument to determine loading of Pt in the Pt/CMK-3 product.

Electrochemical measurements

The electrochemical tests were conducted on an AutoLab PGSTAT 30 potentiostat. A three-electrode electrochemical cell with Pt plate as counter electrode, Ag/AgCl as reference electrode and glassy carbon (GC) electrode with an area of 0.20 cm^2 as working electrode was used. The GC electrode was polished to a mirror finish with a 0.05 μm suspension before each experiment. The catalyst ink was composed of 5.0 mg Pt/OMC, 800 μL ethanol, 100 μL H_2O and 100 μL 0.5 wt% Nafion solution, 20 μL of which was pipetted onto the top surface of GC electrode and dried at 60 ºC for 1 hr. Before each test, the electrolyte was purged with N_2 for electrochemical surface area evaluation and methanol oxidation. All the potentials reported were relative to normal hydrogen electrode (NHE).

Results and discussion

It is known that polymerization of FA, the carbon precursor, precedes carbonization. The condensation polymerization is catalyzed by acids, e.g. oxalic acid (OA), with moderate heating at 80 ºC.[19] At 160 ºC, cross-linking of poly-furfuryl alcohol (PFA) occurs. Gradual pyrolysis reactions occur at higher temperatures.[19] The platinum precursor, H_2PtCl_6, is acidic and hygroscopic. Its function as catalyst for FA polymerization has, to our best knowledge, not been reported. Platinum precursor catalyzed FA polymerization is a key to enable this reverse order synthetic route. We observed ready polymerization of FA in a beaker when contacted with H_2PtCl_6 added into the beaker at room temperature. During subsequent heating in the carbonization step, H_2PtCl_6 thermally decomposes to platinum nanoparticles between 220 - 500 ºC with emission of hydrogen chloride and chlorine.[20] The FA that polymerized around H_2PtCl_6 acts as a protecting agent to prevent agglomeration and growth of Pt nanoparticles at elevated temperatures. This PFA protection agent gradually turns into carbon and forms an integral part of the electrocatalyst.

Feasibility of the CPDP route can be demonstrated by characterization of the final structure of the supported electrocatalyst denoted as Pt/CMK3-CPDP. The dispersion and uniformity of Pt nanoparticles in the CMK3 can be clearly seen in the TEM image of Fig. 1. It is remarkable that the dispersion and small size of the Pt particles can be preserved during carbonization at 700 ºC for 3 hrs. Also, the structure of the carbon CMK3 was shown to be highly ordered with a hexagonal symmetry from Fig. 1b and its inset. It confirms that H_2PtCl_6 can function well not only as a catalyst for FA polymerization and also as a Pt precursor in the prepartion of the dispersed Pt nanoparticles in CMK3, and the PFA initiated from H_2PtCl_6 nanoparticles can efficiently prevent the growth of Pt nanoparticles during carbonization.

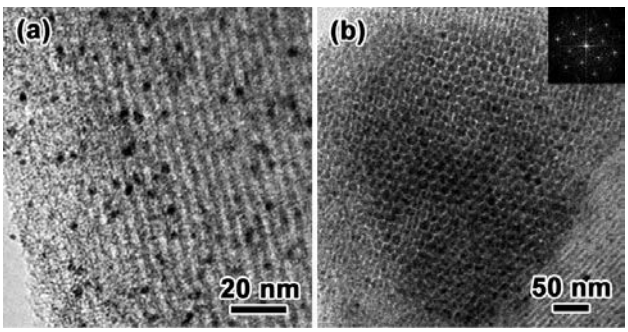

Fig. 1 TEM images Pt/CMK3-CPDP at two different magnifications and projections: (a) higher magnification and (b) along the [100] direction with corresponding Fourier diffractogram (inset).

The effectiveness and superiority of the CPDP route are demonstrated by the resulting Pt/CMK3 structure having i) higher loading and more uniform dispersion of Pt; ii) better carbon structure with higher surface area and pore volume; and iii) higher electrochemical activity compared to Pt/CMK3 synthesized via the conventional ethylene glycol (EG) method.[8]

Fig. 2 compares the TEM images of Pt/CMK3 prepared by the EG method and that of the CPDP method. More uniform particle size and better dispersion are evident in Pt/CMK3-CPDP. Some large particles of 10 nm are observed in Pt/CMK3-EG whereas those in Pt/CMK3-CPDP are uniform at 3.3 nm. There are clusters of Pt nanoparticles near the edge of CMK3 in Fig. 2a (lower left corner) but the dispersion of particles in Fig. 2b, and in Fig. 1 are uniform. The particle size distribution in the inset of Fig. 2b shows particle size between 2 to 5 nm. A micrometer scale TEM image of Pt/CMK3-CPDP at low magnification in Fig.

3 also shows good dispersion of Pt nanoparticles without agglomeration. It may be deduced that Pt nanoparticles in Pt/CMK3-CPDP are uniformly distributed inside the mesopores of CMK3, while many Pt nanoparticles are on the outer surface of CMK3 in Pt/CMK3-EG .

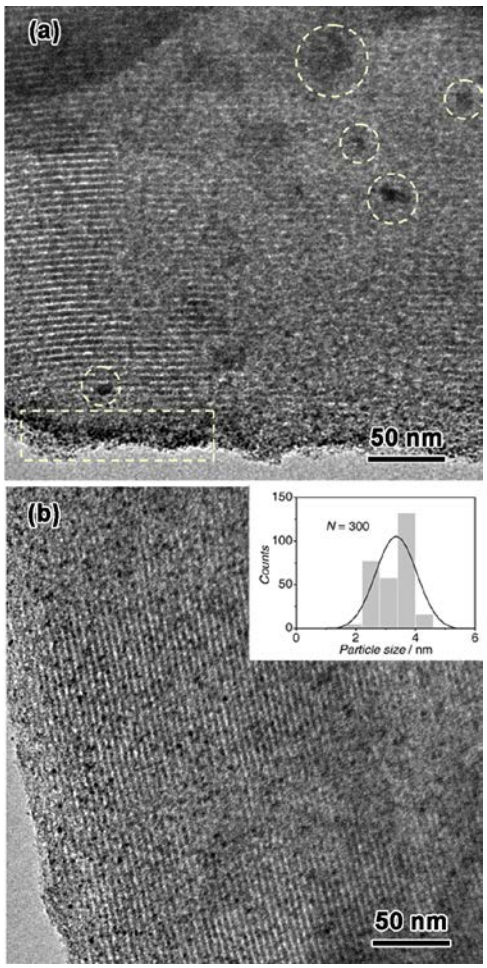

Fig.2 TEM images (a) Pt/CMK3-EG, (b) Pt/CMK3-CPDP. The enclosed regions in (a) indicate poor dispersion of Pt nanoparticles.

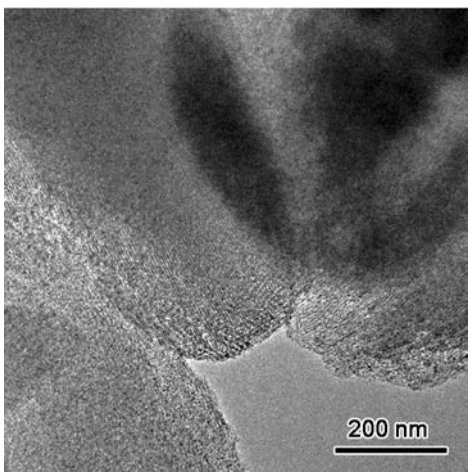

Fig. 3 Low magnification TEM image of Pt/CMK3-CPDP.

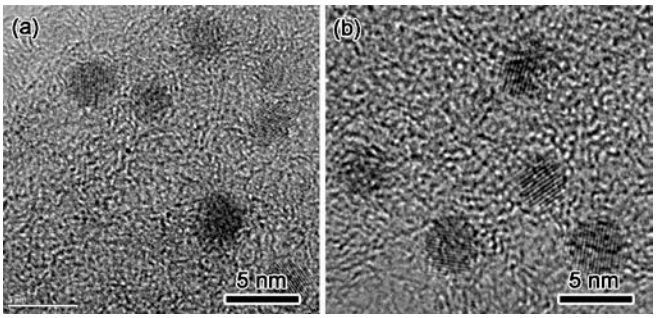

Fig. 4 HRTEM images of (a) Pt/CMK3-EG, and (b) Pt/CMK3-CPDP.

The HRTEM images of the Pt nanoparticles in the two structures show similar and well-developed lattices in Fig. 4a and b, respectively. In the two synthetic routes, the same amount of platinum precursors was used. The Pt loadings in Pt/CMK3-EG and Pt/CMK3-CPDP measured by thermal gravimetric analysis, were 8.4 wt% and 10.8 wt%, respectively. A 50 wt% Pt loading via the CPDP route can be achieved with good dispersion, as shown in the TEM image of Fig. 5. The Pt loading was also determined by thermal gravimmetry analysis (TGC) in air. The weight loss versus temperature profiles are shown in Fig. 6. The silanol groups on SBA-15 could be negatively charged and therefore repel and resist the penetration of $PtCl_6^{-2}$ ions. The SBA-15 was prepared under acidic conditions in presence of 1.6 M HCl. The point of zero charge of the silica[21] is *pH* 2 whereas the *pH* of H_2PtCl_6 solution is between 1.0 and 2.0. The silica groups in SBA-15 should be H terminated and not hindering the penetration and adsorption of the Pt. High loadings of Pt, such as the 50% loading in Fig. 5, can therefore be achieved.

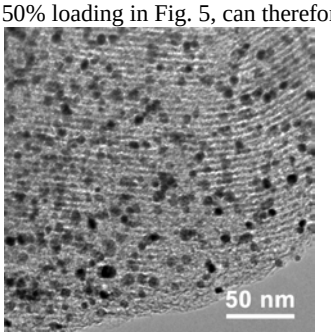

Fig. 5 TEM image of Pt/CMK3-CPDP with a loading of 50 wt% Pt..

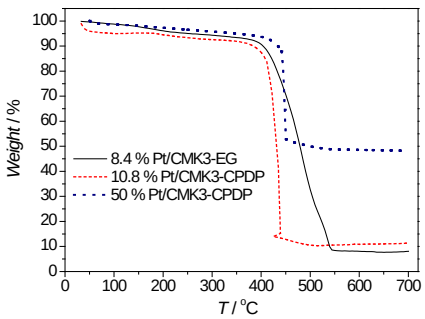

Fig. 6 TGA curves of to determine Pt loading in the three Pt loaded carbon samples.

This journal is © The Royal Society of Chemistry [year]

Despite loaded with more Pt, the Pt/CMK3-CPDP structure has higher surface area and pore volume than Pt/CMK3-EG, as characterized by nitrogen sorption in Fig. 7. The structural parameters of the silica template, the resulting Pt-free, and Pt loaded carbon structures are compared in Table 2.

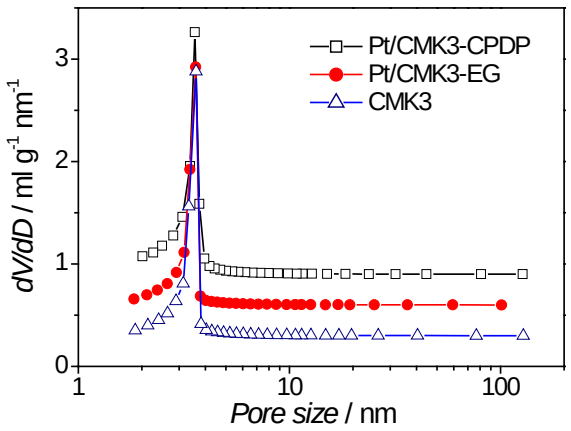

Fig. 7 Nitrogen sorption determined pore size distributions of Pt-free CMK3 carbon, and Pt/CMK3 prepared by CPDP and EG methods.

Table 2 Structural parameters of SBA-15, CMK3 and Pt loaded CMK3. (S_{BET}, surface area from BET method; V, pore volume calculated at a single point of $P/P_o = 0.97$; D_p, average pore size.)

Structure	SBET, m^2/g	V, ml/g	D_p, nm	Pt loading m/m	ECSA m^2/gPt
SBA-15	537	1.04	6.6		
CMK3	1186	1.30	3.6		
Pt/CMK3-EG	1024	1.23	3.5	8.4%	67.4
Pt/CMK3-CPDP	1355	1.31	3.6	10.8%	78.4

It is counter-intuitive that the 10.8 wt% Pt loaded Pt/CMK3-CPDP structure can have a higher surface area than the Pt-free CMK3 structure. This suggests a different carbon meso-structure resulting from the different steps of the synthetic routes, e.g. retention of carbon during silica removal. While the carbon precursor and carbonization temperature are identical, the H_2PtCl_6 catalyst can be a more effective catalyst for FA polymerization than oxalic acid. There appears to be better interfacing and filling of carbon precursor in silica pores via H_2PtCl_6 catalyzed polymerization. When conventional FA polymerization catalysts are used, heating is required to initiate polymerization. This leads to some losses of FA through evaporation. The ability of H_2PtCl_6 to catalyze FA polymerization at low temperature preserves FA monomers and allows more thorough and compact filling of FA into the silica pore. The diameters of the mesopores are similar in the three carbon structures as tabulated in Table 2.

The pore size distribution in Pt/CMK3-CPDP shows a sharp peak at 3.6 nm, similar to those of Pt/CMK3-EG and Pt-free CMK3, as shown in Fig. 7. The mesopores of Pt/CMK3-CPDP retains the long range order of the SBA-15 template, as shown in the TEM image along the [100] direction in Fig. 1b and the corresponding Fourier diffractogram (inset). The resulting Pt/CMK3-EG, Pt/CMK3-CPDP, and Pt-free CMK3 carbons show similar distributions of G bands and D bands in the Raman spectra in Fig. 8. This suggests the same ratio of graphitic to amorphous carbons and similar hydrophilic/hydrophobic character in the three carbons. It appears that the addition of Pt precurors before carbonization does not affect the atomic scale structure of carbon which is mostly affected by the carbonization temperature.

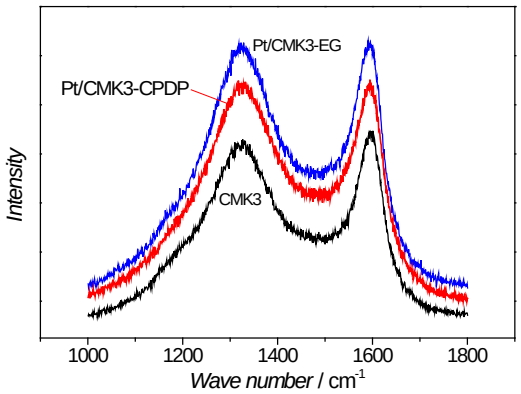

Fig. 8 Raman spectra of Pt-free CMK3 carbon, and Pt/CMK3 prepared by CPDP and EG methods.

Electrochemical surface area (ECSA) of Pt/CMK3-EG and Pt/CMK3-CPDP was evaluated in 0.1 M $HClO_4$ at 5 mV/s and the corresponding CVs are shown in Fig. 9. The ECSAs were calculated by integrating the charges between 0.05 and 0.25 V in the hydrogen desorption region, based on an ideal monolayer hydrogen adsorption charge of 0.21 mC/cm^2 on polycrystalline Pt. In Table 2, the ECSA of Pt/CMK3-CPDP is 16 % higher than that of Pt/CMK3-EG.

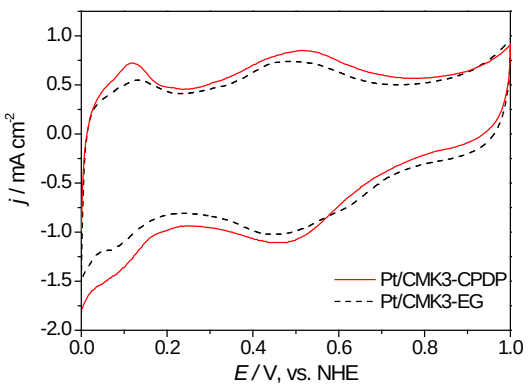

Fig. 9 Cyclic voltammograms of Pt/CMK3 prepared by CPDP and EG methods in 0.1 M $HClO_4$ at 5 mV/s.

A big contrast of electrocatalytic activity is observed in methanol oxidation in $HClO_4$. The Pt/CMK3-CPDP electrocatalyst gives more than two times, the methanol oxidation current compared to that of Pt/CMK3-EG, as shown in Fig. 10. It is noticeable that the current peek position of

Pt/CMK3-CPDP in the forward scan is negatively shifted in comparison with Pt/CMK3-EG, suggesting higher activity.

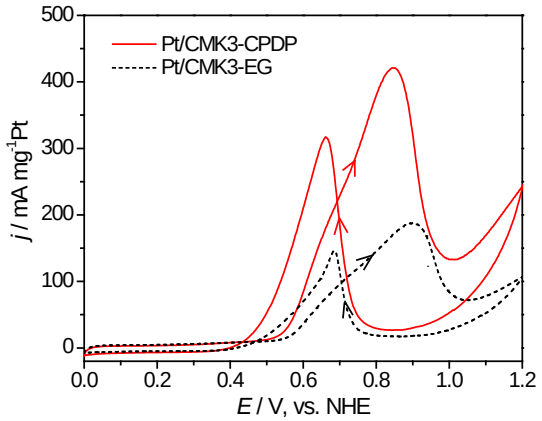

Fig. 10 Cyclic voltammograms of Pt loaded carbons in 0.1 M $HClO_4$ containing 1.0 M methanol at 5 mV/s. The Pt loading is about 10 wt% as in Table 2.

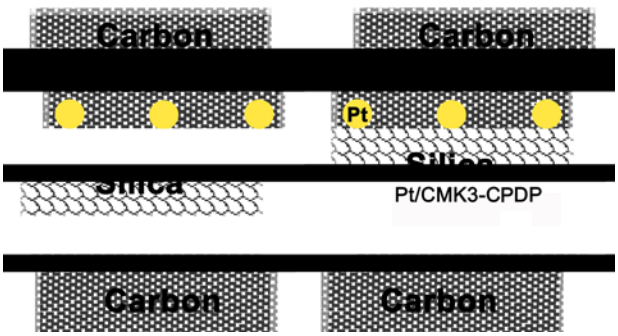

Fig. 11 Platinum-carbon interfaces in Pt/CMK3-CPDP and Pt/CMK3-EG structures.

In addition to better dispersion of Pt, higher pore volume, and surface area of the carbon structure, the higher electrochemical activity may be due to an optimum Pt/C interface. At an intermediate step of the CPDP process, the Pt nanoparticles are sandwiched at the silica/carbon interface but are more embedded into carbon substrate which forms around the Pt nanoparticles. The removal of silica in the final step will expose the Pt nanoparticles which are embraced by the carbon support, as shown in the upper panel of Fig. 11. On the other hand, for the conventional synthetic route shown in the lower panel, the Pt nanoparticles were deposited onto an existing carbon substrate with less carbon/platinum integration. There can be differences in the platinum/carbon interfaces of the two structures, as shown in Fig. 11, and may lead to difference in catalytic activity and stability.

Conclusions

We demonstrate here a feasible, effective, and preferred route of synthesizing mesoporous supported Pt electrocatalysts with high electrochemical performance. While an example is drawn from the CMK3 structure, the underlying chemistry, particular the H_2PtCl_6 catalyzed FA polymerization can be extended and generalized to make other mesoporous carbons supported Pt electrocatalysts. Studies can be made to extend the synthetic method for preparation of other mixed metal nanoparticles, e.g. PtRu. The envisaged unique Pt/C interface in the CPDP route for stability deserves further investigations.

Acknowledgements

Financial supports from GRF Awards 700208, 700209P, the University of Hong Kong SRT and UDF on Initiative for Clean Energy and Environment Research are acknowledged. TEM was performed in the Electron Microscopy Unit of University of Hong Kong. Raman Microscopy was performed in Dr. T. Zhang's group in HKU Civil Engineering and TGA was performed in Prof. X. Lu's group in Nanjing University of Technology. KYC received a Croucher Foundation Senior Research Fellowship and Universitas 21 Fellowship.

Notes and references

Department of Chemistry, The University of Hong Kong, Pokfulam Road, Hong Kong. Fax: +852 28597971, E-mail: hrsccky@hku.hk.

1 J. Zhang, K. Sasaki, E. Sutter and R. R. Adzic, *Science* 2007, **315**, 220.
2 N. Tian, Z. Y. Zhou, S. G. Sun, Y. Ding and Z. L. Wang, *Science* 2007, **316**, 732.
3 S. Jun, S. H. Joo, R. Ryoo, M. Kruk, M. Jaroniec, Z. Liu, T. Ohsuna and O. Terasaki, *J. Am. Chem. Soc*. 2000, **122**, 10712.
4 S. H. Joo, S. J. Choi, I. Oh, J. Kwak, Z. Liu, O. Terasaki and R. Ryoo, *Nature* 2001, **412**, 169.
5 W. C. Choi, S. I. Woo, M. K. Jeon, J. M. Sohn, M. R. Kim and H. J. Jeon, *Adv. Mater*. 2005, **17**, 446.
6 J. Ding, K. Y. Chan, J. Ren and F. Xiao, *Electrochim. Acta* 2005, **50**, 3131.
7 J. S. Yu, S.Kang, S. B. Yoon and G. Chai, *J. Am. Chem. Soc*. 2002, **124**, 9382.
8 K. Y.Chan, J. Ding, J. Ren, S. Cheng and K. Y. Tsang, *J. Mater. Chem*. 2004, **14**, 505.
9 M. L. Liu, C. C. Huang, M. Y. Lo and C. Y. Mou, *J. Phys. Chem. C* 2008, **112**, 867.
10 D. Zhao, J. Feng, Q. Huo, N. Melosh, G. H. Fredrickson, B. F. Chmelka and G. D. Stucky, *Science* 1998, **279**, 548.
11 V. R. Stamenkovic, B. Fowler, B. S. Mun, G. Wang, P. N. Ross, C. A. Lucas and N. M. Markovic, *Science* 2007, **315**, 493.
12 F. Kleitz, S. H. Chui and R. Ryoo, *Chem. Commun*. 2003, 2136.
13 B. Fang, N. K. Chaudhari, M. S. Kim, J. H. Kim and J. S. Yu, *J. Am. Chem. Soc*. 2009, **131**, 15330.
14 Y. Wang, J. Ren, K. Deng, L. Gui and Y. Tang, *Chem. Mater*. 2000, **12**, 1622.
15 C. Bock, C. Paquet, M. Couillard, G. A. Botton and B. R. MacDougall, *J. Am. Chem. Soc*. 2004, **126**, 8028.
16 M. H. Chen, Y. X. Jiang, S. R. Chen, R. Huang, J. L. Lin, S. P. Chen and S. G. Sun, *J. Phys. Chem. C* 2010, **114**, 19055.
17 X. Zhang and K. Y. Chan, *Chem. Mater*. 2003, **15**, 451.
18 S. H. Liu, R. F. Lu, S. J. Huang, A. Y Lo, S. H. Chien and S. B. Liu, *Chem. Commun*. 2006, 3435.
19 N. Guigo, A. Mija, L. Vincent and N. Sbirrazzuoli, *Phys. Chem. Chem. Phys*. 2007, **9**, 5359.
20 A. E. Schweizer and G. T. Kerr, *Inorg. Chem*. 1978, **17**, 2326.
21. A. Vinu, V. Murugesan, W. Böhlmann, M. Hartmann, *J. Phys. Chem*. B 2004, **108**, 11496.

This journal is © The Royal Society of Chemistry [year]